

The radial velocity trail from the giant planet orbiting τ Boötis

Matteo Brogi¹, Ignas A. G. Snellen¹, Remco J. de Kok², Simon Albrecht³, Jayne Birkby¹ and Ernst J. W. de Mooij^{1,4}

¹*Leiden Observatory, Leiden University, Postbus 9513, 2300RA Leiden, The Netherlands*

²*SRON, Sorbonnelaan 2, 3584 CA Utrecht, The Netherlands*

³*Department of Physics, and Kavli Institute for Astrophysics and Space Research, Massachusetts Institute of Technology, Cambridge, Massachusetts 02139, USA*

⁴*Department of Astronomy and Astrophysics, University of Toronto, 50 St. George Street, Toronto, ON M5S 3H4, Canada*

The giant planet orbiting τ Boötis was among the first extrasolar planets to be discovered through the reflex motion of its host star¹. It is one of the brightest known and most nearby planets with an orbital period of just a few days. Over the course of more than a decade, measurements of its orbital inclination have been announced² and refuted³, and have subsequently remained elusive⁴⁻⁸ until now. Here we report on the detection of carbon monoxide absorption in the thermal day-side spectrum of τ Boötis b. At a spectral resolution of $R \sim 100,000$, we trace the change in the radial velocity of the planet over a large range in phase, determining an orbital inclination of $i = 44.5 \pm 1.5^\circ$ and a true planet mass of $5.95 \pm 0.28 M_{\text{Jup}}$. This result extends atmospheric characterisation to non-transiting planets. The strong absorption signal points to an atmosphere with a temperature that is decreasing towards higher altitudes. This is a stark contrast to the temperature inversion invoked for other highly irradiated planets^{9,10}, and supports models in which the absorbing compounds believed to cause such atmospheric inversions are destroyed by the ultraviolet emission from the active host star¹¹.

We observed τ Boötis for 3x6 hours during the nights of April 1, 8, and 14, 2011, with the Cryogenic InfraRed Echelle Spectrograph (CRIRES¹²) at the Nasmyth A focus of the Very Large Telescope UT1, located at the European Southern Observatory on Cerro Paranal, Chile. Targeting the planet almost continuously between orbital phase $0.37 < \phi < 0.63$, we collected 452 spectra at a resolution of $R \sim 100,000$ in the wavelength range 2287-2345 nm, centred on the 2-0 R-branch of carbon monoxide. We used the ESO CRIRES data pipeline for the basic data reduction and the extraction of the one-dimensional spectra. We subsequently extracted the signal of the planet using purpose-built algorithms, similar to those utilised for high-dispersion transit spectroscopy of

HD209458b¹³, which are described in detail in the Supplementary Information (SI-2). The most critical step in this analysis is the removal of telluric features caused by the Earth's atmosphere, which completely dominate our spectra. This can be achieved without destroying the planetary signature only because the signal from the planet moves significantly in wavelength during our observations, due to its large change in radial velocity along the orbit.

We cross-correlated each of the 452 extracted and processed spectra with a CO template (described in SI-5.1), and subsequently aligned and combined all the cross-correlation functions, assuming a range of values for the maximum orbital radial velocity of the planet, K_p . Figure 1 shows the combined cross-correlation signal as function of K_p , corresponding to a wide range in orbital inclinations. We detect a 6σ absorption signal at $K_p = (110.0 \pm 3.2) \text{ km sec}^{-1}$, at the systemic velocity of $-16.4 \text{ km sec}^{-1}$, which is within the uncertainties of that of the host star¹⁴ τ Boötis. The distributions of the values of the cross-correlated time series for points in the planet trail and out of the planet trail are shown in Figure 2. A detailed discussion on the noise properties of the cross-correlated time series and on the significance level of this detection is presented in SI-3. Figure 3 shows the radial velocity trail of the planet in CO over the full phase range of our observations. Combining the measured K_p with the maximum radial velocity of the host star, $K_s = (0.4664 \pm 0.0033) \text{ km sec}^{-1}$ (see SI-4), yields a star/planet mass ratio of 235.8 ± 7.1 . With a host stellar mass¹⁵ of $M_s = (1.34 \pm 0.05) M_{\text{Sun}}$ we derive a planetary mass of $M_p = (5.95 \pm 0.28) M_{\text{Jup}}$. In addition, using Kepler's Third Law, we determine a planet orbital inclination of $i = (44.5 \pm 1.5)^\circ$. Note that orbital solutions to the long-term monitoring of the radial velocity variations of the host star show a modest preference¹⁶ for a slightly eccentric orbit with eccentricity $e = (0.023 \pm 0.015)$. However, the combination of our planet radial velocity data and a reanalysis of the stellar data in the literature shows no evidence for an eccentric orbit (see SI-4). We therefore adopt a circular orbit for τ Boötis b in our analysis.

Spectro-polarimetric observations^{14,17} of τ Boötis show that the host star exhibits strong differential rotation, with a period ranging from $P_{\text{rot}} = 3.0$ to 3.9 days from the equator to the poles. It indicates that the stellar rotation at intermediate latitudes is synchronised with the planet's orbital period ($P = 3.312$ days). If we assume that the stellar rotation axis is aligned with the normal to the orbital plane of the planet, the projected rotational velocity¹⁶ of the star, $v \sin(i) \sim 15 \text{ km sec}^{-1}$, combined with a stellar radius¹⁵ of $R_s = (1.46 \pm 0.05) R_{\text{Sun}}$ and our measurement of i , indeed corresponds to a stellar rotational period of $P_{\text{rot}} = 3.3$ days, matching the planet's orbital period. Therefore, in addition to synchronization, it suggests that the orbital plane and the plane of stellar rotation are not significantly misaligned. We would like to point out that a large fraction of the hot

Jupiters around hot stars ($T_{\text{eff}} > 6250$ K) such as τ Boötis, whose orbital alignment can be measured via the Rossiter-McLaughlin effect, exhibit strong misalignments^{18,19}. However, most of the massive planets ($M_p > 3 M_{\text{Jup}}$) are found in more aligned orbits²⁰, and τ Boötis b does not break this trend.

Our observations at high spectral resolution are only sensitive to narrow spectral features, because of the particular data reduction necessary to remove the telluric contamination. Due to the high opacity at the wavelengths of molecular transitions, these narrow features probe the atmosphere at lower pressures than the surrounding continuum. The probed pressures are directly linked to the Volume Mixing Ratio (VMR) of CO, but the depth of the absorption features in the emitted planet spectrum depends on the relative temperatures at the levels of the continuum and CO lines. This means that there is a strong degeneracy between the temperature-pressure (T/P) profile of the planet atmosphere, and the VMR of CO. We compare our data with a range of models, in order to constrain the CO abundance and the T/P profile (see SI-5.2). We obtain a lower limit of the CO VMR by using the adiabatic lapse rate ($dT/d\log_{10}(p) \sim 1000$ K at these temperatures), which is the maximum temperature gradient of a planet atmosphere before it becomes unstable to convection. An additional uncertainty is that the size of τ Boötis b is unknown, because it is a non-transiting planet. Since the average radius of the seventeen transiting hot-Jupiters currently known²¹ with $3 M_{\text{Jup}} < M_p < 9 M_{\text{Jup}}$ is $1.15 R_{\text{Jup}}$, we assume this value for the planet. When we set the temperature of the atmospheric layer in which the continuum is formed to $T = 2000$ K (near the expected dayside equilibrium temperature for a planet without energy redistribution to the night-side), and use an adiabatic lapse rate, we require a CO VMR of 10^{-5} to match the observed signal. If we assume a temperature of $T = 1650$ K for the continuum photospheric layer (near the dayside equilibrium temperature for a planet with perfect redistribution to its night-side), under similar adiabatic conditions, a CO VMR of 10^{-4} is required. Note that this result is consistent with the metallicity of the host star, corresponding to a CO VMR of $\sim 10^{-3}$. We do not detect spectral features from methane or water vapour above a significance of 2σ , and we use our atmospheric models to derive upper limits to the relative abundances of these molecules of $\text{VMR}(\text{CH}_4)/\text{VMR}(\text{CO}) < 1$ and $\text{VMR}(\text{H}_2\text{O})/\text{VMR}(\text{CO}) < 5$ at a 90% confidence level.

Photometric observations of hot Jupiters with the Spitzer Space Telescope have been interpreted as suggestive of thermal inversions, characterized by molecular features in emission rather than in absorption, of which HD209458b is the best-studied example. These inversions are likely fuelled by absorption of stellar radiation in a high-altitude absorbing layer. In such a model a thermal inversion is more likely to occur in the most highly irradiated planets, for which indeed

some evidence exists²². The planet τ Boötis is more strongly irradiated than HD209458b. However, it is clear that τ Boötis does not exhibit a strong thermal inversion over the pressure range probed by our observations, since we see the CO signal in absorption. Although the exact pressure range probed depends on the CO abundance, the inversion layer invoked to explain the emission spectrum of HD209458b encompasses such a wide range in atmospheric pressures that it is evident that τ Boötis does not have a HD209458b-type thermal inversion. Interestingly, the host star of τ Boötis b exhibits a high level of chromospheric activity, and it has been recently suggested that hot-Jupiters orbiting active stars are less likely to have thermal inversions¹¹, because the strong UV radiation that accompanies chromospheric activity destroys the absorbing compound at high altitude, which would otherwise be responsible for the thermal inversion.

These observations show that high-resolution spectroscopy from the ground is a valuable tool for a detailed analysis of the temperature structure and molecular content of exoplanet atmospheres. The used technique not only reveals its potential for transmission spectroscopy¹³, but also for dayside spectroscopy, meaning that atmospheric characterization is no longer constrained to transiting planets alone. Detection of different molecular bands will further constrain the relative molecular abundances and temperature-pressure profiles. In addition, tracing the signal along the orbit will reveal the planet phase function, which is linked to its global atmospheric circulation. Measuring this for different molecules may reveal changes between a planet's morning and evening spectrum driven by photo-chemical processes. Furthermore, molecular line profiles, in both dayside and transmission spectra, can potentially show the effects of a planet's rotational velocity, and unveil whether these hot Jupiters are indeed tidally locked.

References

1. Butler, R. P., Marcy, G. W., Williams, E., Hauser, H. & Shirts, P. Three new “51-Pegasi-type” planets. *Astrophys. J.* **474**, L115-L118 (1997)
2. Collier Cameron, A., Horne, K., Penny, A. & James, D. Probable detection of starlight reflected from the giant planet orbiting τ Boötis. *Nature* **402**, 751-755 (1999)
3. Collier Cameron, A., Horne, K., James, D., Penny, A. & Semel, M. τ Boo b: not so bright, but just as heavy. in *Proceedings of IAU Symposium 202: Planetary Systems in the Universe* (eds Penny, A. J., Artymowicz, P., Lagrange, A.-M. & Russell, S.) 75-77 (Astronomical Society of the Pacific, 2004)
4. Leigh, C., Collier Cameron, A., Horne, K., Penny, A. & James, D. A new upper limit on the

- reflected starlight from τ Bootis b. *Mon. Not. R. Astron. Soc.* **344**, 1271-1282 (2003)
5. Charbonneau, D., Noyes, R. W., Korzennik, S. G., Nienson, P. & Jha, S. An upper limit on the reflected light from the planet orbiting the star τ Bootis. *Astrophys. J.* **522**, L145-L148 (1999)
 6. Wiedemann, G., Deming, D. & Bjoraker, G. A sensitive search for methane in the infrared spectrum of τ Bootis. *Astrophys. J.* **546**, 1068-1074 (2001)
 7. Lucas, P. W., Hough, J. H., Bailey, J. A., Tamura, M., Hirst, E. & Harrison, D. Planetpol polarimetry of the exoplanet systems 55 Cnc and τ Boo. *Mon. Not. R. Astron. Soc.* **393**, 229-244 (2009)
 8. Rodler, F., Kürster, M. & Henning, T. τ Boötis b: hunting for reflected starlight. *Astron. Astrophys.* **514**, 23-30 (2010)
 9. Burrows, A., Budaj, J. & Hubeny, I. Theoretical spectra and light curves of close-in extrasolar giant planets and comparison with data. *Astrophys. J.* **678**, 1436-1457 (2008)
 10. Fortney, J. J., Lodders, K., Marley, M. S. & Freedman, R. S. A unified theory for the atmospheres of the hot and very hot Jupiters: two classes of irradiated atmospheres. *Astrophys. J.* **678**, 1419-1435 (2008)
 11. Knutson, H. A., Howard, A. W. & Isaacson, H. A correlation between stellar activity and hot-Jupiter emission spectra, *Astrophys. J.* **720**, 1569-1576 (2010)
 12. Käufl, H. U. *et al.* CRIRES: a high resolution infrared spectrograph for ESO's VLT, *Proc SPIE* **5492**, 1218-1227 (2004)
 13. Snellen, I. A., de Kok, R. J., de Mooij, E. J. W. & Albrecht, S. The orbital motion, absolute mass and high-altitude winds of exoplanet HD209458b, *Nature* **465**, 1049-1051 (2010)
 14. Donati, J.-F. *et al.* Magnetic cycles of the planet-hosting star τ Bootis. *Mon. Not. R. Astron. Soc.* **385**, 1179-1185 (2008)
 15. Takeda, G. *et al.* Structure and evolution of nearby stars with planets. II. Physical properties of \sim 1000 cool stars from the SPOCS catalog. *ApJS* **168**, 297-318 (2007)
 16. Butler, R. P. *et al.* Catalog of nearby exoplanets. *Astrophys. J.* **646**, 505-522 (2006)
 17. Catala C., Donati, J.-F., Shkolnik, E., Bohlender, D. & Alecian, E. The magnetic field of the planet-hosting star τ Bootis. *Mon. Not. R. Astron. Soc.* **374**, L42-L46 (2007)
 18. Winn, J. N., Fabrycky, D., Albrecht, S. & Johnson, J. A. Hot stars with hot Jupiters have high obliquities. *Astrophys. J.* **718**, L145-L149 (2010)
 19. Johnson, J. A. *et al.* HAT-P-30b: a transiting hot Jupiter on a highly oblique orbit. *Astrophys. J.* **735**, 24-31 (2011)
 20. Hébrard, G. *et al.* Observation of the full 12-hour-long transit of the exoplanet HD 80606b. Warm-Spitzer photometry and SOPHIE spectroscopy. *Astron. Astrophys.* **516**, 95-109 (2010)

21. Schneider, J., Dedieu, C., Le Sinader, P., Savalle, R. & Zolotukhin, I. Defining and cataloguing exoplanets: the exoplanet.eu database. *Astron. Astrophys.* **532**, 79-90 (2011)
22. Knutson, H. A., Charbonneau, D., Burrows, A., O'Donovan, F. T. & Mandushev, G. Detection of a temperature inversion in the broadband infrared emission spectrum of TrES-4. *Astrophys. J.* **691**, 866-874 (2009)

Acknowledgements We thank the ESO support staff of the Paranal Observatory for their help during the observations. Based on observations collected at the European Southern Observatory (186.C-0289). S.A. acknowledges support by a Rubicon fellowship from the Netherlands Organisation for Scientific Research (NWO), and by NSF grant no. 1108595 "Spin-Orbit Alignment in Binary Stars".

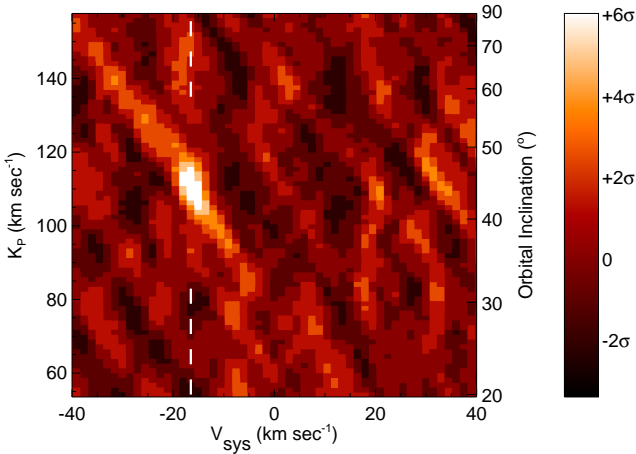
Author Contributions M.B. led the observations and data analysis, and co-wrote the manuscript. I.S. conceived the project, contributed to the analysis and co-wrote the manuscript. R.d.K. constructed the planet atmosphere models. S.A. conducted the MCMC orbital analysis. J.B., E.d.M., R.d.K., and S.A. discussed the analyses, results, and commented on the manuscript.

Author Information The authors declare no competing financial interests. Correspondence and request for materials should be addressed to M.B. (e-mail: brogi@strw.leidenuniv.nl). Reprints and permissions information is available at www.nature.com/reprints.

Figure 1. CO signal in the dayside spectrum of exoplanet τ Boötis b. Colour scale plot of the carbon monoxide signal as function of heliocentric velocity on the x -axis, and the maximum radial velocity of the planet K_p on the y -axis. The latter translates to an orbital inclination as indicated by the scale on the right side. Lighter colours indicate CO in absorption. A clear signal at a 6.2σ level is visible at the system velocity of τ Boötis ($-16.4 \text{ km sec}^{-1}$), as indicated by the vertical dashed line, for a maximum planet velocity of $K_p = (110.0 \pm 3.2) \text{ km sec}^{-1}$. This corresponds to an orbital inclination $i = (44.5 \pm 1.5)^\circ$ and to a planet mass of $M_p = (5.95 \pm 0.28) M_{\text{Jup}}$. The signal is obtained by cross-correlating a template spectrum of CO lines with the CRIRES/VLT spectra, which were each shifted in wavelength using the planet's ephemeris assuming a K_p . This to compensate for the changing Doppler effect caused by the change in the planet radial velocity over the large range in phase. The significance of the signal and the properties of the cross-correlated noise are discussed in the Supplementary Information.

Figure 2. Comparison of in-trail and out-of-trail cross-correlation values. Distributions of the values of the cross-correlated time series for points in the planet trail (grey) and out of the trail (black). The error bars denote the square root of the number of data points in each bin (1σ). The two distributions clearly deviate, with the in-trail distribution shifted to lower pixel values due to the planet signal. A Welch t-test on the data rejects the hypothesis that the two distributions are drawn from the same parent distribution at the 6σ level.

Figure 3. The orbital trail of carbon monoxide absorption. On panel **a**, the signature of CO in absorption is visible as a sinusoidal trace around the heliocentric radial velocity of τ Boötis from $+80 \text{ km sec}^{-1}$ at phase 0.37, to -80 km sec^{-1} at phase 0.63. On panel **b**, the data are shifted to the reference-frame of τ Boötis b, after subtracting the planet radial velocity computed assuming a circular orbit and a system inclination of 44.5° : here the planet signal is recovered as a vertical trace around $v_{\text{rest}} = 0 \text{ km sec}^{-1}$. A comparison between the observed trail and artificially generated data with the same noise properties is shown in the Supplementary Information (Fig. S4).



Distribution of cross-correlation values

